Photocatalysis

International Edition: DOI: 10.1002/anie.201509744
German Edition: DOI: 10.1002/ange.201509744

A Crystalline Copper(II) Coordination Polymer for the Efficient Visible-Light-Driven Generation of Hydrogen

Xi-Yan Dong, Mei Zhang, Ru-Bo Pei, Qian Wang, Dong-Hui Wei, Shuang-Quan Zang, Yao-Ting Fan, and Thomas C. W. Mak*

Abstract: *A crystalline coordination polymer (CP) photocatalyst (Cu-RSH) which combines redox-active copper centers with photoactive rhodamine-derived ligands remains stable in acid and basic solutions from pH 2 to 14, and efficiently catalyzes dihydrogen evolution at a maximum rate of 7.88 mmol g^{-1} h^{-1} in the absence of a mediator and a co-catalyst. Cyclic voltammetry, control experiments, and DFT calculations established that copper nodes with open coordination sites and favorable redox potentials, aided by spatially ordered stacking of rhodamine-based linkers, account for the high catalytic performance of Cu-RSH. Emission quenching, time-resolved fluorescence decay, and transient photocurrent experiments disclosed the charge separation and transfer process in the catalytic system. The present study demonstrates the potential of crystalline copper CPs for the practical utilization of light.*

Sunlight-driven splitting of water into hydrogen is one of the most promising scenarios for sustainable energy consumption. The development of highly efficient, inexpensive noble-metal-free photocatalysts is a prerequisite, but faces many difficult challenges. Coordination polymers (CPs) that combine functional organic ligands with metal centers/clusters (secondary building units, SBUs) have become promising candidates for photoharvesting and the photocatalytic splitting of water.[1–4] The so-far reported CPs for the hydrogen evolution reaction (HER) rely primarily on a limited number of inert Zr-, Al-, Ti-, and Cr-based SBUs as a result of their stability under harsh catalytic conditions.[2] Moreover, they primarily act as supports to host known catalysts that participate in the catalytic reaction, with noble metal Pt particles representing the majority of these catalysts.[2,3] Developing completely Pt-free and stable CP photocatalysts using redox-active metals, such as Fe, Co, Ni, and Cu in combination with photoactive organic ligands would present viable alternatives for transforming sunlight into chemical energy.[1,4]

[*] Dr. X.-Y. Dong, M. Zhang, R.-B. Pei, Q. Wang, D.-H. Wei, Prof. S.-Q. Zang, Prof. Y.-T. Fan, Prof. T. C. W. Mak
College of Chemistry and Molecular Engineering
Zhengzhou University
Zhengzhou 450001 (China)
E-mail: zangsqzg@zzu.edu.cn
Prof. T. C. W. Mak
Department of Chemistry and Center of Novel Functional Molecules
The Chinese University of Hong Kong
Shatin, New Territories, Hong Kong SAR (China)

Supporting information for this article is available on the WWW under http://dx.doi.org/10.1002/anie.201509744.

Copper is an earth-abundant and relatively low-cost material that is also biologically relevant, for example, in photosynthesis and respiration.[5,6] The Cu^{II} state has well-defined coordination chemistry and can undergo diverse redox reactions (reduction to Cu^{I} or Cu^{0} and oxidation to Cu^{III} or Cu^{IV}), and the potential of the states can be fine-tuned over a broad range by varying the coordination sphere for the redox reaction.[6] Currently, only a few copper complexes have been used for the electrocatalytic reduction[7a] and oxidation of water.[7b] Although crystalline copper CPs are appealing as photocatalysts for the reduction of water, no example has been reported to date.

Incorporating well-established fluorescent dye groups, such as porphyrin-, Ru^{II}-bpy- (bpy = 2,2′-bipyridine), and viologen-based ligands, into organic linkers can lead to photoactive CPs.[8–11] The highly ordered arrangement of dye species in crystalline CPs is expected to enhance their inherent excellent optical absorption and emission, modulate the reactivity and potentials of intrinsically active metal nodes or SBUs,[9] as well as funnel electron transport[10] and transfer energy,[11] all of which are vital in photochemical reactions. As yet, the eminent dye rhodamine has not been exploited as the organic linker of photoactive CPs. Previously, we and other workers have designed various salicylaldehyde rhodamine hydrazone derivatives as fluorescent probes for metal ions, such as Cu^{2+}, Fe^{3+}, and Al^{3+},[12] among which carbonyl O, imino N, and phenol O atoms provide a three-membered chelating site to form molecular complexes. Anchoring carboxylate groups on the appropriate position of the salicylaldehyde to form a rhodamine-based linker will extend the aforementioned simple molecular complexes into higher-dimensional CPs, which may produce unexpected and desirable functional properties that arise from the more well-organized assembly compared to a simple molecular complex.

We first designed and synthesized a new rhodamine-based carboxylate linker H_2RSH by using rhodamine 6G, hydrazide, and 3-formyl-4-hydroxybenzoic acid (see Scheme S1 and Figure S1 in the Supporting Information), and then reacted it with Cu^{2+} ions to form the one-dimensional (1D) CP $[Cu(RSH)(H_2O)]_n$ (Cu-RSH; Figure 1). This combination of the photoactive rhodamine-based ligand with redox-active Cu^{2+} ions in the highly ordered crystalline structure efficiently photocatalyzed the splitting of water into hydrogen, and Cu-RSH is the first example of a copper-based CP for the visible-light-driven production of hydrogen.

The solvothermal reaction of $CuCl_2 \cdot 2H_2O$ and H_2RSH (the synthesis of the ligand (H_2RSH) is presented in Scheme S1, its crystalline structure is presented in Figure S1,

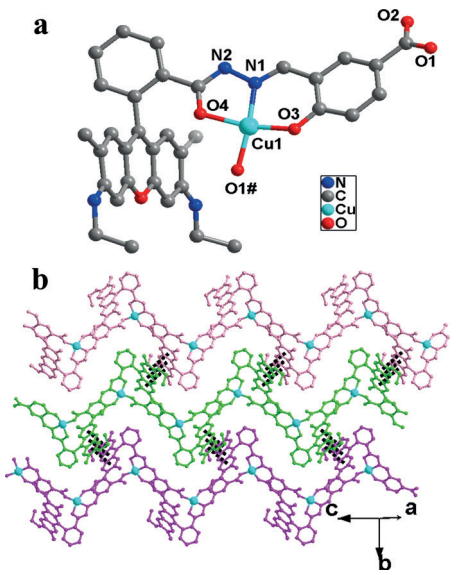

Figure 1. a) Perspective view of the coordination environment of the Cu^{II} center in Cu-RSH. Symmetry code #: *x*, 1.5−*y*, 0.5+*z*. b) View of the packing of zigzag chains in the crystal structure of Cu-RSH. The black dashed bonds represent π-π interactions between the xanthene moieties of adjacent chains. (The separations between aromatic ring centers are 3.647, 3.647, and 3.684 Å.)

and crystal data are listed in Table S1 in the Supporting Information) in a mixed solvent of *N*,*N*-dimethylformamide (DMF) and H_2O produced green blocklike crystals of Cu-RSH. Single-crystal structure analysis revealed that Cu-RSH crystallizes in the monoclinic space group $P2_1/c$ (Table S1). As shown in Figure 1, the asymmetric unit consists of one Cu^{2+} center and one RSH^{2-} ligand; the presence of one lattice water molecule in the formula was determined by thermogravimetric analysis (TGA, Figure S2) and elemental analysis. Each copper(II) center has a distorted square-planar coordination geometry, being surrounded by a phenol O atom of the 3-formyl-4-hydroxybenzoic acid unit, a ketone O atom, and an imine N atom from one RSH ligand, together with a carboxylate O atom from an adjacent RSH ligand (Figure 1 a; selected bond lengths and angles of Cu-RSH are listed in Table S2). Analysis of Cu-RSH by X-ray photoelectron spectroscopy (XPS) showed that the binding energies of the Cu $2p_{3/2}$ and Cu $2p_{1/2}$ levels were 934.1 and 953.9 eV, respectively (Figure S3), which suggests that the Cu center exists in the +2 oxidation state.[13] The carboxylate groups extend the basic structural unit into a wavelike chain structure, with such chains being joined together through π-π interactions (centroid-to-centroid distances: 3.647, 3.647, and 3.684 Å) between the xanthene moieties of adjacent chains to form a layer (Figure 1 b). These layers are packed through intermolecular C−H···π hydrogen-bonding associations (separation between C atom and the centroid of benzene ring: 3.422 Å; Figure S4) to form a three-dimensional supramolecular structure (Figure S5).

The powder X-ray diffraction (PXRD) patterns confirmed the phase purity of Cu-RSH (Figure S6). The morphological and structural integrity of the crystals of Cu-RSH were unchanged after immersing batches of the crystals in aqueous acid (pH 2, HCl) and basic (pH 14, KOH) solutions, as well as in common organic solvents (ethanol, acetone, or acetonitrile), for three days at room temperature, and at 180 °C for 12 h (Figure S6). To our knowledge, the majority of CPs built up from Cu^{2+} ions lack hygroscopic as well as acid/alkali resistance.[14] The remarkable stability of Cu-RSH is very rare for CPs based on divalent metal cations,[14] which enables it to serve as an acid- and base-tolerant catalyst, such as in water-splitting reactions.

The UV/Vis/near-IR diffuse diffraction spectrum (Figure S7) revealed that, compared with the free ligand H_2RSH, the absorption of Cu-RSH exhibited an increased intensity and extended far into the near-infrared (NIR) range, even to 1400 nm. These properties are likely related to the opening of the spiro rings of the rhodamine 6G units,[12] d-d transitions of the Cu^{2+} ions,[15] π-π stacking, and ligand-to-metal charge transfer.[16] Although the spiro ring of the rhodamine 6G unit of the organic linker opens, solid-state Cu-RSH is nonfluorescent, likely because the paramagnetic Cu^{2+} ions accept electrons and energy from the excited states of the rhodamine 6G units and quench their emission.[12]

One-dimensional coordination polymers have been prepared as gels, fibers, nanocrystals, and microspheres for catalysis and other applications.[17] Cu-RSH could be highly dispersed in aqueous ethanol in the form of particulates of several hundred nanometers in length by ultrasonication, as evident from a photograph of a solution containing Cu-RSH, dynamic light scattering (DLS) measurements, and SEM images (Figure S8).

In natural photosynthesis, several dyes cooperatively absorb sunlight and transfer photoexcited charges to a single reaction center.[4] In our experiments, alcohol-soluble Eosin Y (EY) was introduced as a photosensitizer in the photocatalytic system to combine with the rhodamine species of the linker for light harvesting. The optimized system contained alcohol-soluble EY and triethanolamine (TEOA; 10 % v/v) as a hole scavenger in a mixed solvent of EtOH/H_2O (3:1) at pH 13 (Figures S9–S13). Under optimized conditions, Cu-RSH was highly active for the production of H_2, with an average rate of hydrogen production of 7.88 mmol g^{-1} h^{-1}, and a maximum of 197.4 μmol in the first 5 h of irradiation by visible light ($\lambda \geq 420$ nm). The catalytic efficiency of Cu-RSH is one of the highest of the reported Pt-free CP photocatalysts for generating H_2 from water (Table S3).[1–4] In addition, no H_2 was detected in the dark or in the absence of Cu-RSH under the measured conditions, which shows that Cu-RSH is essential for an efficient photochemical reaction. Cu-RSH is also active in purely aqueous systems, from which the detected H_2 yield was 29.6 μmol after 5 h of irradiation (Figure 2). The visible-light ($\lambda \geq 420$ nm) quantum efficiency of about 4 % is the highest reported for a CP-catalyzed reduction of water (Figure S14).[1a] The recovered Cu-RSH retained its structure and its catalytic activity (Figures S15 and S16).

Titration studies showed that the introduction of Cu-RSH (0.76 μmol) into an aqueous ethanol solution of photosensitizer EY (3.07×10^{-5} M) resulted in a significant decrease in the band intensity of the EY emission ($\lambda = 546$ nm), with the quenching efficiency amounting to 82 % (Figure 3 a), thus

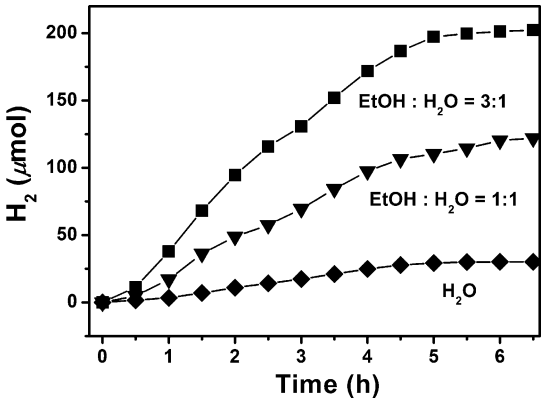

Figure 2. Effect of the volume ratio of EtOH/H_2O on the photocatalytic production of H_2 in the presence of 5 mg Cu-RSH in 15 mL of solution containing 10% TEOA (v/v) and 10 mg EY (5.13×10^{-4} M) at pH 13 in an inert atmosphere.

indicating electron transfer from EY* (the excited state) to Cu-RSH.[18] Concurrently, the emission maximum was red-shifted by 7 nm (from $\lambda = 546$ nm to 553 nm) at Cu-RSH concentrations of 2.2×10^{-4} M (Figure 3a). As both the light absorber EY and the rhodamine-based linker of Cu-RSH contain highly conjugated xanthene moieties and the sub-micrometer diameter particulates of the catalyst were well-dispersed in the catalytic system, EY molecules might have

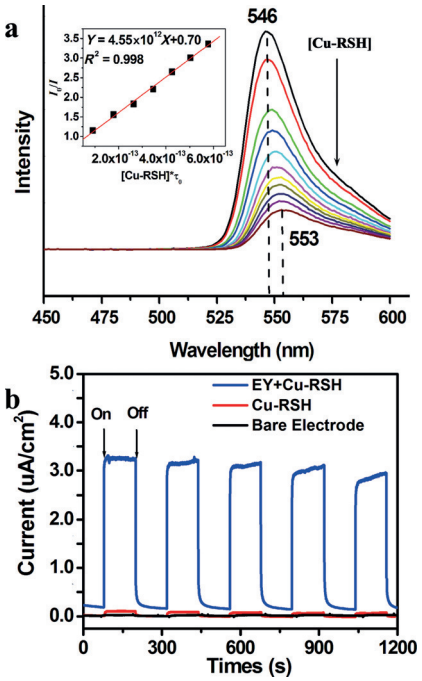

Figure 3. a) Emission spectra of EY as a function of Cu-RSH. Inset: Stern–Volmer plot for the photoluminescence quenching of EY by Cu-RSH. Inset: Stern–Volmer plot for the photoluminescence quenching of EY by Cu-RSH. b) Transient photocurrent/time profiles of the bare glassy carbon electrode (black), pristine Cu-RSH (red), EY + Cu-RSH (blue), which were coated on the glassy carbon electrode with Nafion in a KCl electrolyte (0.1 mol L^{-1}) at a bias of 0.0 V, with and without irradiation with visible light ($\lambda \geq 420$ nm).

adhered to the surface of the catalyst through a noncovalent π-π interaction, which is expected to funnel electrons from the photoexcited EY to Cu-RSH. The process led to a more efficient separation of the photogenerated electrons, thus suppressing the combination of electrons and holes that would result in undesired radiative transition, and is responsible for the red-shift in the emission wavelength of EY.[19,20] Additionally, the EY emission (540–640 nm, $\lambda_{max} = 546$ nm) overlapped with the absorption of Cu-RSH (Figure S7). Therefore, resonance energy transfer (RET) from EY* to Cu-RSH possibly also occurred.[20] Linear fitting of a Stern–Volmer plot gives an apparent rate constant (k_q) of 4.5×10^{12} $M^{-1}s^{-1}$ for oxidative quenching by Cu-RSH, which is a relatively large value (inset in Figure 3a).[18–20] The addition of TEOA as a sacrificial electron donor reductively quenches the EY emission with a k_q value of 3.5×10^{8} $M^{-1}s^{-1}$, which is four orders of magnitude less than the oxidative quenching by Cu-RSH. Furthermore, the position of the EY emission maximum was not affected by the addition of TEOA (Figure S17). When the concentration of the catalyst and TEOA is taken into account, the chance of an oxidative pathway involving Cu-RSH is much higher than that of a reductive path involving TEOA. Therefore, the electron obtained by the catalyst most likely comes from photoexcited EY. Additionally, the lifetime (3.62 ns) of the excited state of EY decreased to 3.35 ns upon addition of Cu-RSH (Figure S18), which also indicates the transfer of photogenerated electrons from the photosensitizer to Cu-RSH.[18,19]

Current/time curves under irradiation with visible light at a bias of 0.0 V (Figure 3b) demonstrated that the electrode modified by pristine Cu-RSH had a small photocurrent response (0.11 μA cm^{-2}) in KCl (0.1 mol L^{-1}), thus confirming that electron transfer occurs from Cu-RSH to the glassy carbon electrode. This finding is consistent with the low catalytic activity without the photosensitizer. However, a dramatically enhanced photocurrent was observed on the electrode modified by EY + Cu-RSH (3.3 μA cm^{-2}), which decayed slowly. This result indicated an improvement in the charge transport from the excited state of EY to Cu-RSH and then to the surface of the working electrode.[21] These findings provide direct evidence of electron transfer from the excited state of EY to Cu-RSH, and is in good agreement with the results of the steady-state and transient-state emission of EY quenching by Cu-RSH.

Control experiments were carried out to provide insight into the catalytic mechanism and evaluate the contribution of metal centers and their outer coordination sphere to H_2 production. First, two Cu-RSH analogues, $Al(HRSH)_2Cl(H_2O)_4$ (Al-RSH) and $Co(HRSH)_2(H_2O)_3$ (Co-RSH), which feature a redox-inactive Al^{3+} and a redox-active Co^{2+} center in place of Cu^{2+}, respectively, were prepared as control materials. Their crystalline structures were determined by SCXRD, TGA, and elemental analysis (Figures S19–S22), and showed that the rhodamine 6G spiro-ring was open, similar to that in Cu-RSH. A major structural difference is that Al-RSH and Co-RSH are simple molecular complexes lacking spatially long-length order. A fresh homogeneous solution (termed as Cu + RSH) containing $CuCl_2$ and H_2RSH (1:1) was then prepared, in which the spiro ring on the

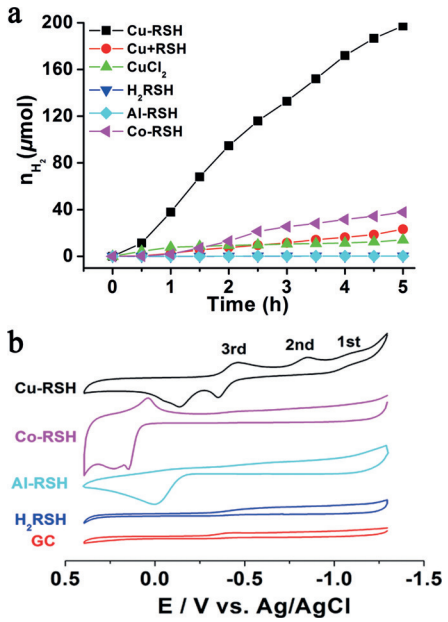

Figure 4. a) Comparison of H_2 evolution from 5 mg samples of Cu-RSH, $CuCl_2$, Cu + RSH, Al-RSH, Co-RSH (containing equivalent metal ions with Cu-RSH), and equal equivalents of ligand (H_2RSH), 10 mg EY, 10% TEOA in a mixed solvent of EtOH/H_2O (3:1), with irradiation by visible light ($\lambda \geq 420$ nm). b) Cyclic voltammograms of Cu-RSH, Co-RSH, Al-RSH, H_2RSH, and the bare glassy carbon (GC) electrode in aqueous KOH solution at pH 13.0. Conditions: glassy carbon as working electrode, Pt plate as counter electrode, and Ag/AgCl reference electrode, scan rate: 100 mV s^{-1} at room temperature.

rhodamine 6G unit was open and the $HRSH^-$ species ligated each Cu^{2+} center in a 1:1 stoichiometry through its carbonyl O, imino N, and phenol O atoms (see UV/Vis absorption titration, Job's method, and the mass spectrometry study in Figures S23–S25, respectively). Next, the hydrogen-evolution efficiencies of $CuCl_2$, the free ligand H_2RSH, Al-RSH, Co-RSH, and Cu + RSH were examined under the same experimental conditions as Cu-RSH. As shown in Figure 4a, the order of photocatalytic activity was as follows: $H_2RSH = Al\text{-}RSH = 0 < CuCl_2 \approx Cu + RSH < Co\text{-}RSH \ll Cu\text{-}RSH$. The ligand H_2RSH and Al-RSH were completely inactive as a result of the lack of active sites. Neither Cu + RSH nor $CuCl_2$ showed meaningful amounts of hydrogen generation. Co-RSH exhibited some catalytic activity in H_2 production, but considerably less than Cu-RSH, which proved to be the most efficient photocatalyst under the tested conditions. The importance of the unique structure of crystalline Cu-RSH is evident by a comparison of Cu + RSH with Cu-RSH. The highly ordered spatial arrangement of the rhodamine-based linkers and metal ions in crystalline Cu-RSH should benefit energy and electron transfer over a long distance.[8–11] This would lead to the rapid transfer of photogenegrated electrons from the excited-state photosensitizer and prompt charge separation efficiency, which could account for the drastically different activities shown by Cu-RSH and Cu + RSH.

The cyclic voltammograms of Cu-RSH, Al-RSH, Co-RSH, and H_2RSH were measured in aqueous KOH solution at pH 13.0 (Figure 4b). Cu-RSH underwent multiple redox changes, and its cyclic voltammogram showed a first quasireversible redox couple at −1.10 V (E_{pc} = cathodic peak potential) and −1.00 V (versus Ag/AgCl; E_{pa} = anodic peak potential), which was assigned to the Cu^I/Cu^0 couple. The second nearly irreversible reduction wave occurred at −0.84 V (versus Ag/AgCl), and the corresponding oxidation waves shifted greatly to −0.36 V, which could be assigned to a Cu^{II}/Cu^I redox process. The relatively large peak splitting ($\Delta E_p = E_{pa} - E_{pc}$) of 0.48 V may be due to distortion of the Cu coordination environment.[22] Therefore, the reduction potential of the excited state of EY* (−1.4 V versus Ag/AgCl)[23] can feasibly reduce Cu^{II} in Cu-RSH to Cu^I or Cu^0. Furthermore, Cu^I/Cu^0, with a more negative reduction potential than the reduction of protons at pH 13 (−0.965 V versus Ag/AgCl), is capable of reducing protons to dihydrogen. The third irreversible redox couple ($E_{pc} = -0.44$ V, $E_{pa} = -0.14$ V versus Ag/AgCl) is likely related to both the metal and the ligand. A subsection sweep over different potential ranges confirmed the redox processes were coupled (Figure S26). The tailor-made redox behavior of Cu-RSH should correlate with the coordination geometry of the copper center and its secondary coordination sphere rendered by the spatially ordered arrangement of the rhodamine-based liands.[6] In contrast, the ligand-based redox waves shifted in the positive direction ($E_{pc} = 0.22$ V, $E_{pa} = 0.037$ V versus Ag/AgCl) in Co-RSH, and only the oxidation waves shifted to approximately 0 V versus Ag/AgCl in Al-RSH, thus indicating that the ligand-related redox potential was sensitive to M^{n+} ions.[24] The free ligand with a closed spiro ring was redox-inactive. Therefore, the proton likely bonded to the open Cu sites to afford a copper hydride species for the release of H_2.[7] This proposed mechanism has been further supported by a computational study (Scheme S2 in Section S9), which demonstrated that the Cu^{II} centers in Cu-RSH could be transformed to Cu^I and then to Cu^0 centers by obtaining electrons from the excited photosensitizer; the Cu^{II} hydrides formed by protonation of Cu^0 species subsequently reacted with H^+ to produce H_2.

The above results highlight the importance of metal ions, coordination sphere, functional ligands, and ordered solid-state structures. A tentative mechanism proposed for the high activity of Cu-RSH for the production of H_2 has been deduced (Figure S27). Photogenerated electrons in EY effectively transfer to Cu-RSH under illumination with visible light, and then the long-length order and conjugated packing of the ligand funnels electrons to a coordinately unsaturated Cu^{2+} center,[8,12] where H_2-evolution reactions occur. The electron donor TEOA scavenges the holes in EY to restore the excited EY to the ground state.

For the first time, a novel crystalline CP with redox-active Cu nodes and a photoactive rhodamine-derived linker has been constructed as a highly effective visible-light photocatalyst for splitting water to H_2. The thermodynamics of the HER, active sites, and the charge separation and transfer process in the three-component photocatalytic system have been elucidated by a series of experiments and theoretical calculations. We believe that our findings can stimulate research on more photoactive dye-based linkers for the assembly of photoactive CPs. In addition to typical Fe, Co, and Ni catalysts, redox-active Cu should merit more attention

for the construction of photocatalysts. Our work opens up new avenues for photocatalytic CPs incorporating functional pigment groups and intrinsically active metal ions/SBUs to achieve solar energy conversion in a molecular material. Modification of the ligand scaffold to optimize the activity of copper complexes for H_2 evolution is in progress.

Acknowledgements

This work was supported by the National Natural Science Foundation of China (No. 21371153) and the Program for Science & Technology Innovation Talents in Universities of Henan Province (13HASTIT008) and the Key Scientific and Technological Project of Henan Province (132102210411) and Zhengzhou University.

Keywords: coordination polymer · copper · dyes/pigments · hydrogen · photochemistry

How to cite: *Angew. Chem. Int. Ed.* **2016**, *55*, 2073–2077
Angew. Chem. **2016**, *128*, 2113–2117

[1] a) T. Zhang, W. Lin, *Chem. Soc. Rev.* **2014**, *43*, 5982; b) S. Kitagawa, R. Kitaura, S. Noro, *Angew. Chem. Int. Ed.* **2004**, *43*, 2334; *Angew. Chem.* **2004**, *116*, 2388; c) Z.-J. Li, X.-B. Li, J.-J. Wang, S. Yu, C.-B. Li, C.-H. Tung, L.-Z. Wu, *Energy Environ. Sci.* **2013**, *6*, 465.

[2] a) M. A. Nasalevich, R. Becker, E. V. Ramos-Fernandez, S. Castellanos, S. L. Veber, M. V. Fedin, F. Kapteijn, J. N. H. Reek, J. I. Vlugt, J. Gascon, *Energy Environ. Sci.* **2015**, *8*, 364; b) S. Pullen, H. Fei, A. Orthaber, S. M. Cohen, S. Ott, *J. Am. Chem. Soc.* **2013**, *135*, 16997; c) C. Wang, K. E. deKrafft, W. Lin, *J. Am. Chem. Soc.* **2012**, *134*, 7211; d) A. Fateeva, P. A. Chater, C. P. Ireland, A. A. Tahir, Y. Z. Khimyak, P. V. Wiper, J. R. Darwent, M. J. Rosseinsky, *Angew. Chem. Int. Ed.* **2012**, *51*, 7440; *Angew. Chem.* **2012**, *124*, 7558.

[3] a) M. Wen, K. Mori, T. Kamegawa, H. Yamashita, *Chem. Commun.* **2014**, *50*, 11645; b) J. He, J. Wang, Y. Chen, J. Zhang, D. Duan, Y. Wang, Z. Yan, *Chem. Commun.* **2014**, *50*, 7063; c) T. Zhou, Y. Du, A. Borgna, J. Hong, Y. Wang, J. Han, W. Zhang, R. Xu, *Energy Environ. Sci.* **2013**, *6*, 3229.

[4] a) X. Jing, C. He, Y. Yang, C.-Y. Duan, *J. Am. Chem. Soc.* **2015**, *137*, 3967; b) J.-S. Qin, D.-Y. Du, W. Guan, X.-J. Bo, Y.-F. Li, L.-P. Guo, Z.-M. Su, Y.-Y. Wang, Y.-Q. Lan, H.-C. Zhou, *J. Am. Chem. Soc.* **2015**, *137*, 7169; c) M. A. Nasalevich, M. van der Veen, F. Kapteijn, J. Gascon, *CrystEngComm* **2014**, *16*, 4919.

[5] C. Dennison, *Coord. Chem. Rev.* **2005**, *249*, 3025.

[6] N. M. Marshall, D. K. Garner, T. D. Wilson, Y.-G. Gao, H. Robinson, M. J. Nilges, Y. Lu, *Nature* **2009**, *462*, 113.

[7] a) P. Zhang, M. Wang, Y. Yang, T. Yao, L.-C. Sun, *Angew. Chem. Int. Ed.* **2014**, *53*, 13803; *Angew. Chem.* **2014**, *126*, 14023; b) M. K. Coggins, M.-T. Zhang, Z. Chen, N. Song, T. J. Meyer, *Angew. Chem. Int. Ed.* **2014**, *53*, 12226; *Angew. Chem.* **2014**, *126*, 12422.

[8] a) C. A. Kent, D. Liu, T. J. Meyer, W. Lin, *J. Am. Chem. Soc.* **2012**, *134*, 3991; b) Y.-N. Gong, T.-B. Lu, *Chem. Commun.* **2013**, *49*, 7711.

[9] K. T. Butler, C. H. Hendon, A. Walsh, *J. Am. Chem. Soc.* **2014**, *136*, 2703.

[10] H.-J. Son, S. Jin, S. Patwardhan, S. J. Wezenberg, N. C. Jeong, M. So, C. E. Wilmer, A. A. Sarjeant, G. C. Schatz, R. Q. Snurr, O. K. Farha, G. P. Wiederrecht, J. T. Hupp, *J. Am. Chem. Soc.* **2013**, *135*, 862.

[11] D. E. Williams, J. A. Rietman, J. M. Maier, R. Tan, A. B. Greytak, M. D. Smith, J. A. Krause, N. B. Shustova, *J. Am. Chem. Soc.* **2014**, *136*, 11886.

[12] a) Y. Fu, X.-J. Jiang, Y.-Y. Zhu, B.-J. Zhou, S.-Q. Zang, M.-S. Tang, H.-Y. Zhang, T. C. W. Mak, *Dalton Trans.* **2014**, *43*, 12624; b) X. Chen, T. Pradhan, F. Wang, J. S. Kim, J. Yoon, *Chem. Rev.* **2012**, *112*, 1910.

[13] J. Yu, J. Ran, *Energy Environ. Sci.* **2011**, *4*, 1364.

[14] a) T. Devic, C. Serre, *Chem. Soc. Rev.* **2014**, *43*, 6097; b) L. Li, R. Matsuda, I. Tanaka, H. Sato, P. Kanoo, H. J. Jeon, M. L. Foo, A. Wakamiya, Y. Murata, S. Kitagawa, *J. Am. Chem. Soc.* **2014**, *136*, 7543; c) D.-Y. Du, J.-S. Qin, S.-L. Li, Z.-M. Su, Y.-Q. Lan, *Chem. Soc. Rev.* **2014**, *43*, 4615.

[15] A. K. Nairn, S. J. Archibald, R. Bhalla, B. C. Gilbert, E. J. MacLean, S. J. Teat, P. H. Walton, *Dalton Trans.* **2006**, 172.

[16] D. Sheberla, L. Sun, M. A. Blood-Forsythe, S. Er, C. R. Wade, C. K. Brozek, A. Aspuru-Guzik, M. Dincă, *J. Am. Chem. Soc.* **2014**, *136*, 8859.

[17] a) T. Kiyonaga, M. Higuchi, T. Kajiwara, Y. Takashima, J. Duan, K. Nagashimac, S. Kitagawa, *Chem. Commun.* **2015**, *51*, 2728; b) W. L. Leong, J. J. Vittal, *Chem. Rev.* **2011**, *111*, 688.

[18] T. Sakai, D. Mersch, E. Reisner, *Angew. Chem. Int. Ed.* **2013**, *52*, 12313; *Angew. Chem.* **2013**, *125*, 12539.

[19] a) C. He, J. Wang, L. Zhao, T. Liu, J. Zhang, C.-Y. Duan, *Chem. Commun.* **2013**, *49*, 627; b) H.-G. Hao, X.-D. Zheng, T.-B. Lu, *Angew. Chem. Int. Ed.* **2010**, *49*, 8148; *Angew. Chem.* **2010**, *122*, 8324.

[20] S. Min, G. Lu, *J. Phys. Chem. C* **2012**, *116*, 19644.

[21] C. Kong, S. Min, G. Lu, *ACS Catal.* **2014**, *4*, 2763.

[22] S. Itoh, N. Kishikawa, T. Suzukib, H. D. Takagi, *Dalton Trans.* **2005**, 1066.

[23] J. Moser, M. Gratze, *J. Am. Chem. Soc.* **1984**, *106*, 6557.

[24] M. Nippe, R. S. Khnayzer, J. A. Panetier, D. Z. Zee, B. S. Olaiya, M. Head-Gordon, C. J. Chang, F. N. Castellano, J. R. Long, *Chem. Sci.* **2013**, *4*, 3934.

Received: October 18, 2015
Published online: December 28, 2015

